

## Tetrathiatriarylmethyl Radicals Conjugated to an RGD-Peptidomimetic

Benoît Driesschaert,<sup>[a,bl]</sup> Philippe Levêque,<sup>[bl]</sup> Bernard Gallez,<sup>[bl]</sup> and Jacqueline Marchand-Brynaert\*<sup>[al]</sup>

**Keywords:** Imaging agents / Radicals / EPR spectroscopy / Peptidomimetics / Density functional calculations

Tetrathiatriarylmethyl (TAM) radicals are favourite spin labels for electron paramagnetic resonance imaging (EPRI). In this work, we report a straightforward synthesis of new TAM radicals bound to an Arg-Gly-Asp (RGD)-peptido-

mimetic known to be a cell-targeting agent. These new radicals are stable in solution, and sensitive to oxygen, and their experimental EPR data is consistent with density functional theory (DFT) calculations.

### Introduction

Electron paramagnetic resonance imaging (EPRI) is an emerging technique that allows researchers to map the distribution of paramagnetic species.<sup>[1]</sup> Compared to the well-known nuclear magnetic resonance imaging (MRI) technique extensively used in clinics, the EPRI technique has the advantages of a higher intrinsic sensitivity and the absence of background. Indeed, as there is no endogenous paramagnetic species in sufficient concentration and with a long enough half-life, with the exception of melanin,<sup>[2]</sup> an exogenous paramagnetic spin label has to be injected for EPRI applications.<sup>[3]</sup> Two classes of water-soluble paramagnetic probes are currently used, namely nitroxide (NR) radicals and tetrathiatriarylmethyl (TAM) radicals. The latter, exemplified by CT-03 or the more hydrophilic compound Ox063 (Figure 1), are better spin probes than nitroxide radicals because of their higher stability in biological media and the lower intrinsic linewidth of their single EPR line, which results in a higher signal-to-noise ratio (signal intensity is inversely proportional to the square of the linewidth).<sup>[4]</sup>

To the best of our knowledge, TAM radicals conjugated to a targeting moiety have not been described in the literature except by ourselves,<sup>[5]</sup> although a few examples of similar conjugates based on nitroxide radicals exist. For instance, NRs have been coupled to arabinogalactan or fatty

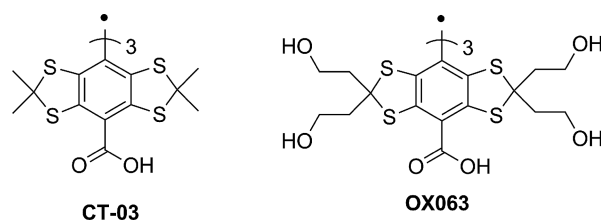


Figure 1. Structures of CT-03 and Ox063.

acid moieties to target liver cells,<sup>[6]</sup> and to peptides for targeting integrins.<sup>[7]</sup>

The highly challenging chemistry of TAM<sup>[8]</sup> radicals could explain this lack of synthetic investment. In this paper, we report the first synthesis of TAM radicals coupled to a peptidomimetic molecule to target the  $\alpha_v\beta_3$  integrin. Integrins are transmembrane receptors that play crucial roles in cell-to-cell and cell-to-matrix adhesion phenomena.<sup>[9]</sup> Specifically, the  $\alpha_v\beta_3$  integrin is overexpressed on the spreading endothelial cells of new capillaries in the angiogenic process linked to tumour growth and development.<sup>[10]</sup> In addition, it is also expressed on certain invasive tumour cells.<sup>[11]</sup> Therefore the  $\alpha_v\beta_3$  integrin has been considered as an appealing target for anticancer therapy (drugs) and cancer diagnosis (probes).<sup>[12]</sup> The  $\alpha_v\beta_3$  integrin interacts with several extracellular matrix proteins through recognition of the RGD (Arg-Gly-Asp) tripeptide sequence.<sup>[13]</sup> RGD-containing cyclic peptides, such as Cilengitide<sup>[14]</sup> (in clinical trials for treatment of glioblastoma) and peptidomimetics of this sequence have been intensively developed as potent antagonists of  $\alpha_v\beta_3$  integrin for therapeutic purposes.<sup>[15]</sup> Some molecules bearing a spacer arm for grafting onto devices or matrices are also used in various biotechnological applications.<sup>[16]</sup>

Guided by the X-ray structure<sup>[17]</sup> of the extracellular part of  $\alpha_v\beta_3$  integrin in complex with Cilengitide, our group has previously designed RGD-peptidomimetics based on the L-tyrosine scaffold (Figure 2). The parent compound (i.e., **1**)

[a] Institute of Condensed Matter and Nanosciences (IMCN), Molecules, Solids and Reactivity (MOST) Université catholique de Louvain Place Louis Pasteur 1, L4.01.02, 1348 Louvain-la-Neuve, Belgium E-mail: jacqueline.marchand@uclouvain.be <http://www.uclouvain.be/en-most.html>

[b] Louvain Drug Research Institute (LDRI), Biomedical Magnetic Resonance Section (REMA) Université catholique de Louvain Avenue Mounier 73, B1.73.08, 1200 Bruxelles, Belgium

Supporting information for this article is available on the WWW under <http://dx.doi.org/10.1002/ejoc.201403049>.

showed an excellent ability to bind isolated human  $\alpha_v\beta_3$  integrin, with an  $IC_{50}$  value of 0.1 nM.<sup>[18]</sup> The derivatives (i.e., **2**) equipped with oligoethylene glycol (OEG) spacer arms retained the antagonist activity ( $IC_{50}$  = 0.3–0.7 nM).<sup>[18]</sup> Moreover, the anchorage of **2** onto the surface of culture substrates allowed a strong adhesion of human endothelial cells and their retention under shear stress.<sup>[19]</sup>

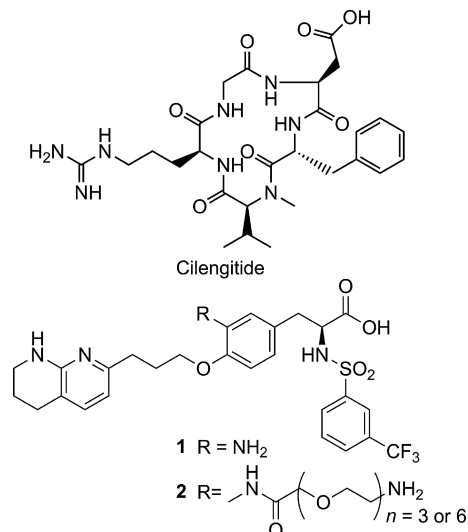


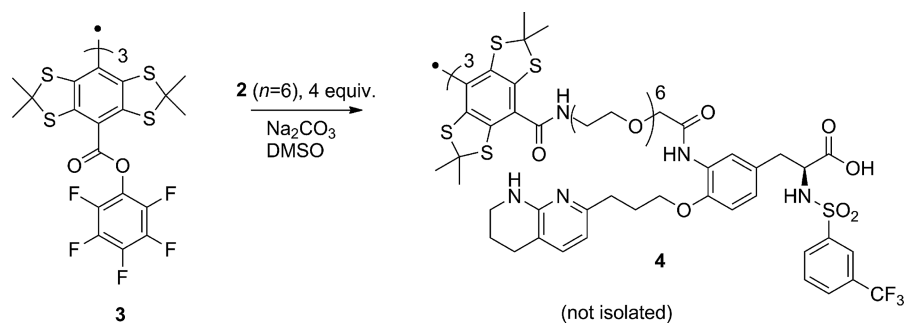
Figure 2. Structures of Cilengitide and (bottom) peptidomimetic developed by our group.<sup>[18]</sup>

## Results and Discussion

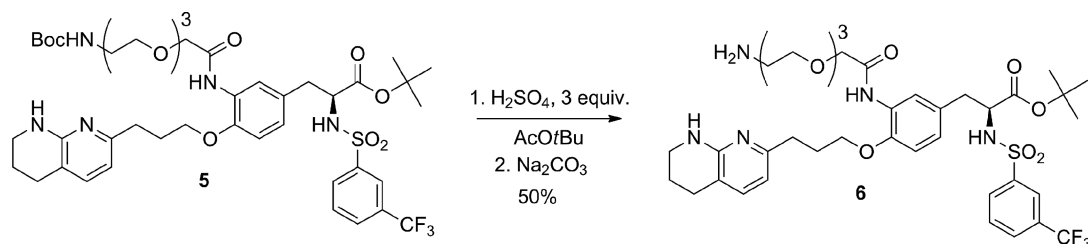
The graftable RGD-peptidomimetic **2** ( $n = 6$ ) was synthesized as described previously.<sup>[20]</sup> Since all the polar functionalities are unprotected, we envisaged as a first strategy

the reaction of **2** with an activated ester of the TAM radical, namely pentafluorophenol triester derivative **3**.<sup>[5]</sup> This activated ester **3** was treated with 4 equiv. of peptidomimetic **2** (bis TFA salt) and Na<sub>2</sub>CO<sub>3</sub> in degassed DMSO (Scheme 1). A change of colour from red to green occurred during the reaction as a result of the coupling of **2** through the terminal primary amine of its OEG spacer. The product (i.e., **4**), featuring three peptidomimetic moieties, was detected in the crude mixture by mass spectrometry (calcd. for [(M + 2)/2]<sup>+</sup> 1821.4931; found 1821.2750). However, we failed to purify this compound by flash chromatography on silica gel, crystallization, or semi-preparative reverse-phase HPLC. This was probably due to the high molecular weight of the compound, and the presence of several acidic and basic functionalities giving polyionic species for all the values of pH we screened for HPLC purification.

To overcome the purification difficulties, an alternative synthetic strategy was envisaged with a double objective. Firstly, to limit the number of ionizable groups, and to allow purification on silica gel, we decided to attach only one peptidomimetic moiety onto the TAM core, and to use an acid-protected form of peptidomimetic **2** ( $n = 3$ ). Secondly, to keep the possibility of analysing the product by nuclear magnetic resonance (NMR) spectroscopy, we chose to use the TAM alcohol instead of the radical for the coupling reaction. Starting from bis-protected intermediate **5**,<sup>[18]</sup> selective Boc (*tert*-butoxycarbonyl) deprotection was carried out by treatment with 3 equiv. of sulfuric acid in *tert*-butyl acetate (Scheme 2).<sup>[21]</sup> Under these particular conditions, amine deprotection was complete, because the resulting amine is stabilised by protonation, while the deprotection of the carboxylic acid is reversible. Indeed, the *tert*-butyl cation, produced from the reaction between *tert*-butyl acetate and sulfuric acid, can re-esterify the carboxylic acid to



Scheme 1. First strategy envisaged for the synthesis of TAM radical bound to peptidomimetic **2**.

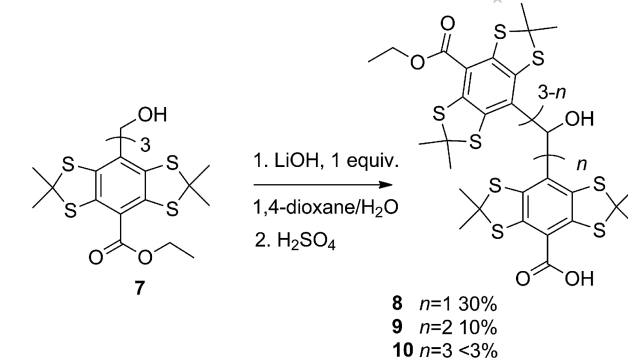


Scheme 2. Selective *N*-Boc deprotection of diprotected peptidomimetic **5**.

give the *tert*-butyl ester. After a basic work-up, the selectively Boc-protected compound (i.e., **6**) was isolated in 50% yield by flash chromatography.

The triethyl ester of TAM alcohol (i.e., **7**) was synthesized using a procedure described in the literature<sup>[22]</sup> with slight modifications; some side-products were identified that have never been reported before (see Supporting Information). Treatment of **7** with just 1 equiv. of aqueous LiOH in refluxing 1,4-dioxane led to the partial, statistical hydrolysis of **7** (Scheme 3). Flash chromatography allowed the recovery of about 40% of the starting material (i.e., **7**), 30% of the desired monohydrolysed compound (i.e., **8**) and 10% of the dihydrolysed compound (i.e., **9**). Due to the high polarity of the trihydrolysed compound (i.e., **10**), it was not recovered from the silica gel column.

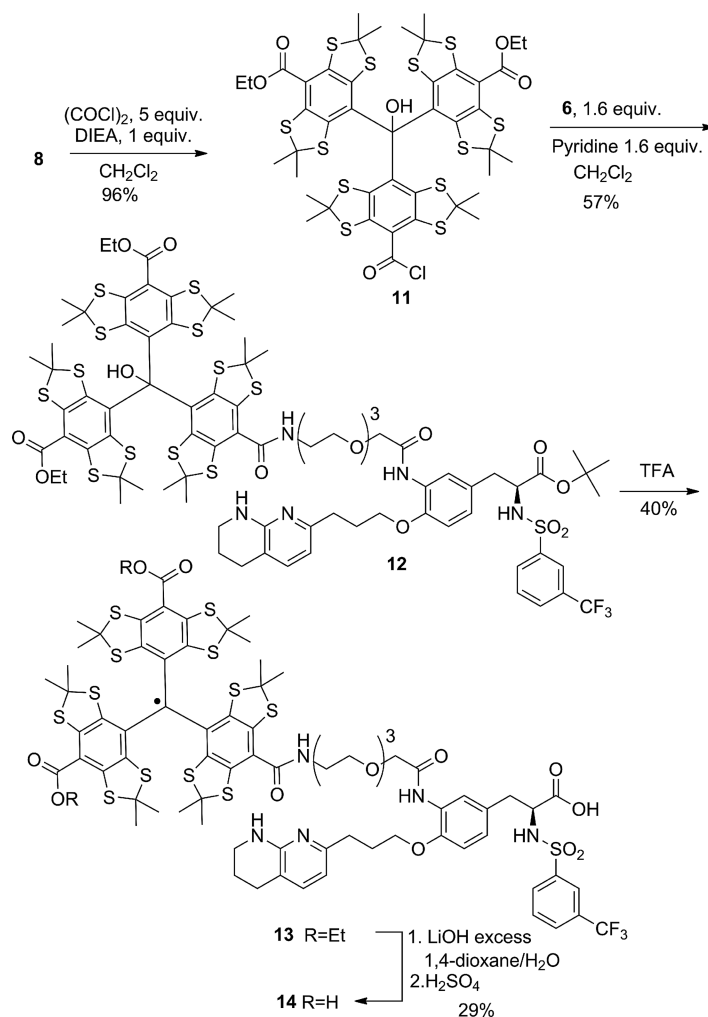
Activation of the monohydrolysed compound was achieved by treating **8** with an excess of oxalyl chloride and 1 equiv. of diisopropylethylamine (DIEA) in dichloromethane (Scheme 4). The acyl chloride (i.e., **11**) was recovered in 96% yield by simple filtration through a short silica gel pad.



Scheme 3. Partial hydrolysis of TAM alcohol **7**.

It is worth noting that no reaction was observed between the trityl alcohol and oxalyl chloride, probably due to the steric protection of the hydroxy group.

In the next step, selectively deprotected peptidomimetic **6** was treated with activated TAM compound **11** in the pres-



Scheme 4. Activation of TAM alcohol **8**, coupling with peptidomimetic **6**, and deprotection of the *tert*-butyl ester with concomitant formation of the TAM radical, followed by hydrolysis of the ethyl esters.

ence of pyridine in dichloromethane. The resulting coupling product (i.e., **12**) was purified by flash chromatography and isolated in 57% yield (Scheme 4). The assignment of the NMR signals of this highly complex molecule was achieved using 2D sequences such as COSY, HMBC, and HMQC (see Supporting Information). Then, treatment of **12** with neat trifluoroacetic acid (TFA) led, simultaneously, to the deprotection of the *tert*-butyl ester and the conversion of the alcohol into the TAM radical to give **13** (Scheme 4). The formation of a tetrathiatriarylmethyl radical by treatment of a tetrathiatriarylmethyl alcohol with neat TFA has been previously reported,<sup>[23]</sup> and the mechanism has been fully explained in a recent publication.<sup>[8c]</sup> The reaction works in the absence of a reductant (like SnCl<sub>2</sub>) because trityl cations can participate in electron-transfer reactions. The production of the radical was accompanied by the formation of an oxidative decarboxylation side-product (the quinone methide).<sup>[8c]</sup> Purification by semi-preparative reverse-phase HPLC allowed the isolation of the pure trityl spin probe bound to the RGD-peptidomimetic moiety (i.e., **13**) in 39% yield. To enhance the hydrophilicity of this new spin label, the two remaining ethyl esters were hydrolysed using excess LiOH. Bis-acid **14** was purified by semi-preparative reverse-phase HPLC to give the final compound in 29% yield (Scheme 4). The relatively low yields of the last two steps can be explained by a loss of material during the HPLC purification (the product fraction was collected only at the maximum of the elution peak to avoid contamination by side-products<sup>[8c]</sup>).

The two new radicals (i.e., **13** and **14**) were isolated in high purity, as shown by their chromatograms obtained under gradient elution (Figure 3). In addition, the radicals are stable in methanol solution at room temperature for at least 48 h (no trace of degradation products could be seen in the HPLC analyses). The pure radicals can be stored for months in the freezer.

For biomedical EPR applications, spin label **14** is more interesting because of its higher hydrophilicity. Its EPR spectrum was recorded at X-band ( $\approx 9.4$  GHz) under anoxic conditions (Figure 4). The spectrum mainly shows a triplet pattern resulting from the hyperfine coupling between the odd electron and the <sup>14</sup>N ( $I = 1$ ) of the amide group. In addition, small peaks corresponding to molecules naturally labelled with <sup>13</sup>C (natural abundance of 1.1%,  $I = 1/2$ ) are also visible.

For highly accurate determination of the hyperfine splitting constant (*hfc*), the spectrum was fitted using the Levenberg–Marquard algorithm, as implemented in Easy-Spin.<sup>[24]</sup> The results are summarized in Table 1.

The assignment of the <sup>13</sup>C satellites was achieved with the help of the intensity ratio and calculation of the isotropic *hfc* ( $A_{iso}$ ). The structure of model radical **15** (Figure 5) was optimized at the UB3LYP/6-31G\* level of theory, and  $A_{iso}$  was calculated at the UB3LYP level of theory with two different basis sets: in the gas phase, and in water using the PCM model (polarizable continuum model; Table 1). Due to its low intensity (1.1% of the total signal), the signal corresponding to the molecule with the central

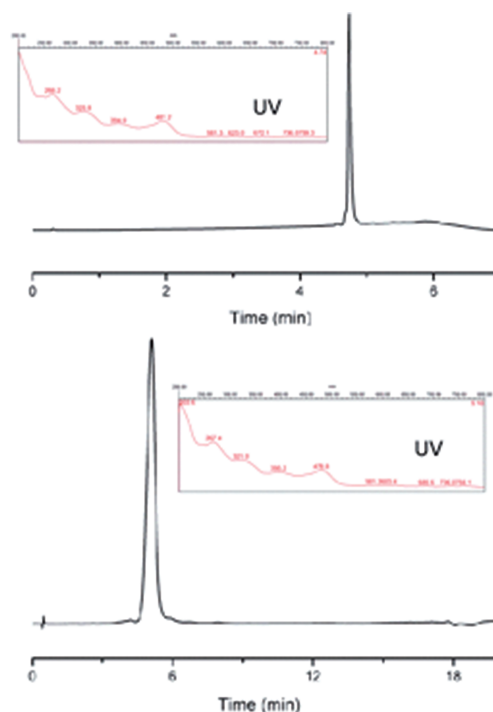


Figure 3. Chromatograms and UV spectra of TAM radicals **13** (upper) and **14** (lower) obtained under gradient elution (see Supporting Information for complete conditions).

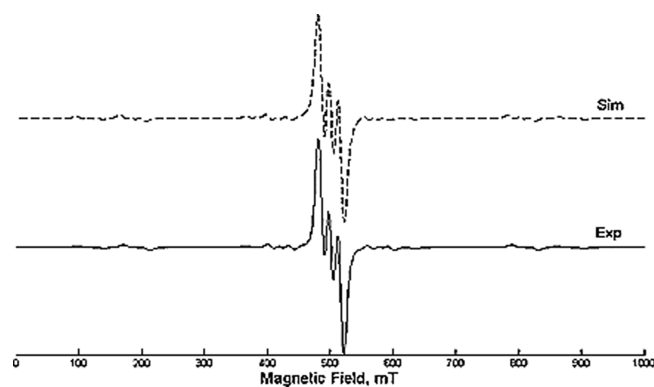


Figure 4. X-band EPR spectrum of **14** in PBS (phosphate-buffered saline)/MeOH (50:50), 0.5 mM under nitrogen. The acquisition settings were: field centre: 3375.36 G, scan range: 15 G, data points: 1024, modulation amplitude: 0.05 G, modulation frequency: 100 KHz, time constant: 20.48, power: 1.272 mW. The fitting parameters are given in the Supporting Information. Exp = experimental spectrum, Sim = simulated spectrum.

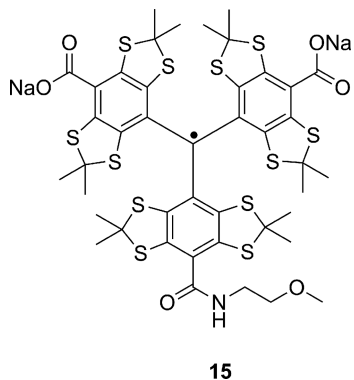
carbon <sup>13</sup>C labelled was not visible, and the spectrum was focussed on the region of the other hyperfine splittings. The hyperfine splitting with the aromatic <sup>13</sup>C was well resolved. The calculated data using the 6-311+G\*\* basis set are in good agreement with the measured data, and are more accurate than those obtained with the 6-31G\* basis set. The difference between the calculated and the experimental <sup>14</sup>N  $A_{iso}$  values could be due to rotation of the amide group at room temperature in solution, which could change the spin density on the nitrogen, and thus the hyperfine coupling

Table 1. Measured and calculated isotropic coupling constant ( $A_{\text{iso}}$ ). The values are given in MHz and in parentheses in  $\mu\text{T}$ .

Nucleus	X-Band	6-31G*[ <sup>a</sup> ]	6-311+G**[ <sup>a</sup> ]	6-311+G** in water[ <sup>a</sup> ]	Degeneracy	Assignment
$^{13}\text{C}$	/[ <sup>b</sup> ]	90.97	53.98	53.80	1	Central C
$^{13}\text{C}$	31.49 (1123.6)	$30.85 \pm 0.14$	$31.64 \pm 0.10$	$31.57 \pm 0.11$	3	1-Aryl
$^{13}\text{C}$	25.43 (907.4)	$29.23 \pm 1.31$	$25.744 \pm 1.74$	$25.54 \pm 1.47$	6	2,6-Aryl
$^{13}\text{C}$	6.41 (228.7)	$7.32 \pm 1.12$	$6.21 \pm 1.10$	$6.32 \pm 1.07$	6	3,5-Aryl
$^{13}\text{C}$	9.38 (334.7)	$12.16 \pm 0.19$	$7.60 \pm 0.11$	$7.71 \pm 0.12$	3	4-Aryl
$^{14}\text{N}$	0.62 (22.1)	0.22	0.15	0.23	1	Amide

[a] The absolute value. [b] The  $A_{\text{iso}}$  value measured for CT-03 was 67.1 MHz.<sup>[25]</sup>

constant. Couplings with the  $^1\text{H}$  ( $I = 1/2$ ) of the amide or the methylene amide were not resolved at X-Band.

Figure 5. Structure of model radical **15**.

Oxygen is a free radical containing two unpaired electrons (in its ground state). It can interact with a free radical to induce relaxation and a line broadening of the EPR signal of the radical. This phenomenon is used to assay oxygenation in vitro and in vivo by EPR.<sup>[3]</sup> The EPR spectrum of **14** was analysed as a Voigt function,<sup>[26]</sup> i.e., the convolution of a Lorentzian function and a Gaussian function resulting from unresolved hyperfine splitting. The Lorentz peak-to-peak ( $\Delta_{\text{LP-P}}$ ) linewidth of radical **14** depends on the

amount of dissolved molecular oxygen in the solution. As shown in Figure 6, there is a linear relationship between the  $\Delta_{\text{LP-P}}$  linewidth and the partial pressure of oxygen ( $p\text{O}_2$ ) ( $0.8 \mu\text{T}/\% \text{O}_2$ ), as is the case for soluble spin labels (trityls, nitroxides).<sup>[3]</sup> Thus, compound **14** could be used as a spin

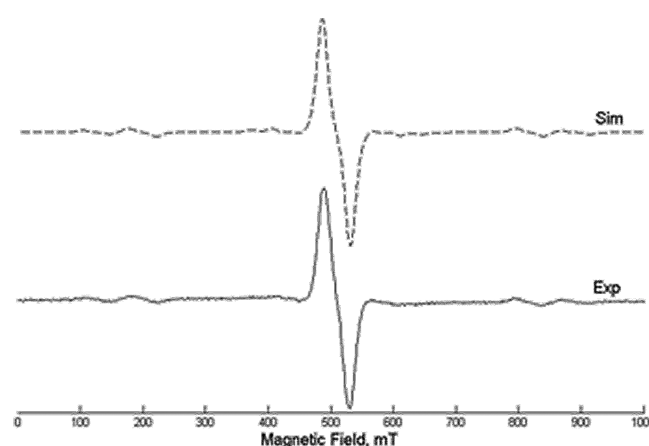
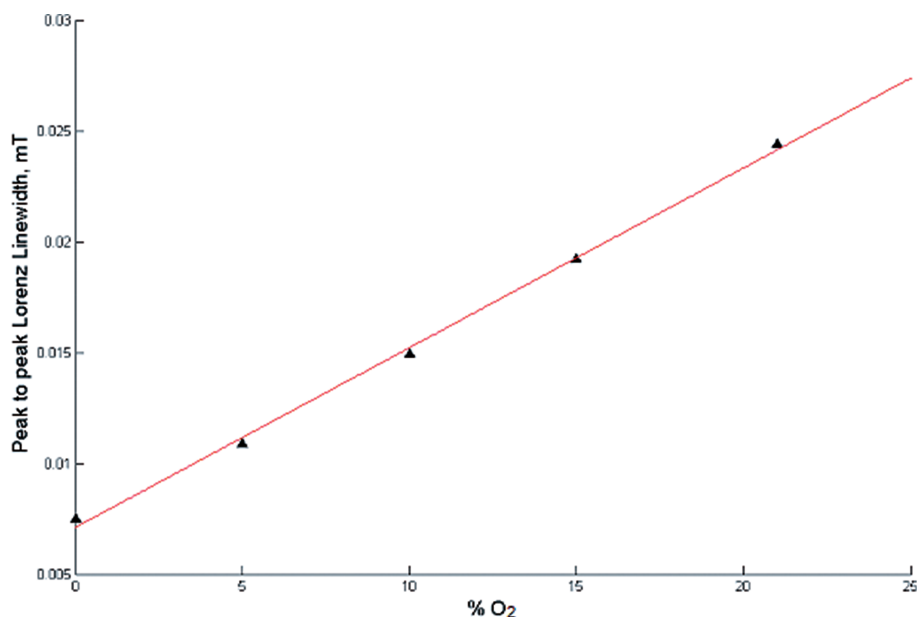


Figure 7. X-band EPR spectrum of **13** in PBS/MeCN (50:50) 5 mm under nitrogen. The acquisition settings were: field centre: 3374.38 G, scan range: 15 G, data points: 1024, modulation amplitude: 0.05 G, modulation frequency: 100 KHz, time constant: 20.48, power: 1.269 mW. The fitting parameters are given in the Supporting Information.

Figure 6. Calibration of the peak-to-peak Lorentz linewidth vs.  $p\text{O}_2$ .

label for EPR oximetry. The less hydrophilic structure **13** shows a similar EPR pattern (Figure 7). However, the resolution of the spectrum is lower, due to additional hyperfine splitting with the methylene protons of the esters. Compound **13** also shows a similar sensitivity to oxygen (data not shown).

## Conclusions

We have synthesized new TAM radicals conjugated to an RGD-peptidomimetic molecule whose antagonist activity against  $\alpha_v\beta_3$  integrin has been demonstrated in previous publications.<sup>[18,19]</sup> This work represents the first example of EPR spin labels linked to a specific recognition motif for a receptor, although probes conjugated to ligands of  $\alpha_v\beta_3$  integrin have already been described in the context of other imaging techniques such as MRI, SPECT (single photon emission tomography), PET (positron emission tomography), and FMT (fluorescence-mediated tomography).<sup>[27]</sup> Generally, RGD-peptides and cyclopeptides are used; RGD-peptidomimetics have been considered in a few cases, as exemplified by the coupling of **2** ( $n = 6$ ) to ultra-small particles of iron oxide (USPIO).<sup>[20]</sup>

The stability of radicals **13** and **14** and their EPR characteristics are adequate for the further development of imaging applications. The success of our synthetic strategy is built on several chemical tricks that can be useful in general for the difficult TAM radical chemistry. By keeping the alcohol group on the trityl core for most of the reaction sequence, we allow accurate characterization of the intermediates by NMR spectroscopy. Moreover, activation of the carboxyl group with oxalyl chloride is an efficient method to produce the acyl chloride in high yield with no alteration of the TAM hydroxy group. In contrast, all attempts to carry out the coupling reaction with in situ activation reagents {BOP [(benzotriazol-1-yloxy)tris(dimethylamino)-phosphonium hexafluorophosphate], carbodiimides} failed (data not shown), even though they are reported to be efficient with the TAM radical.<sup>[28]</sup> Finally, partial hydrolysis of TAM **7** allows isolation of monoacid **8** in 52% yield [based on the recovery of starting material (SM)], and bis-acid **9** in 17% yield (based on the recovery of SM). While **8** was used here to bind only one carrier molecule, compound **9** could be similarly used to link the trityl core to two dedicated entities. Radicals **13** and **14** are sensitive to oxygen, and can be used as spin labels for EPR oximetry. In addition, density functional theory (DFT) calculation of the hfc for radical **15** (model) was in good agreement with the experimental data for radical **14**. The new spin labels are currently being investigated in in vitro assays.

## Experimental Section

**General Remarks:** All commercially available reagents were used as received without further purification. NMR spectra were recorded with a Bruker Avance DPX instrument ( $^1\text{H}$ : 500 MHz;  $^{13}\text{C}$ : 125 MHz). Chemical shifts ( $\delta$ ) are reported in parts per million

(ppm), referenced to NMR solvents, [ $\text{D}$ ]chloroform [ $\delta(^1\text{H}) = 7.27$  ppm,  $\delta(^{13}\text{C}) = 77.2$  ppm], [ $\text{D}_6$ ]dimethyl sulfoxide [ $\delta(^1\text{H}) = 2.50$  ppm,  $\delta(^{13}\text{C}) = 39.52$  ppm]. The following abbreviations are used: s = singlet, br. s = broad singlet, d = doublet, t = triplet, m = multiplet. The atom numbering used for the NMR spectral assignment is given in the Supporting Information. Coupling constants ( $J$ ) are reported in Hertz (Hz). HRMS analysis was carried out at University College London. Analytical HPLC was carried out with a Waters Alliance 2690 separation module equipped with a Waters 2998 photodiode array (PDA) detector. Semi-preparative reverse-phase HPLC was carried out with a Waters 600 Pump equipped with a Waters 486 UV detector, a Waters fraction collector III, and a Hitachi L-7200 HPLC autosampler. EPR spectra were recorded with an X-Band Bruker EMX spectrometer equipped with an ER4119HS resonator; the data were recorded under nonsaturating conditions. Calculations were performed with Gaussian 09.<sup>[29]</sup> Geometry optimization was performed at the UB3-LYP/6-31G\* level, and hfc was calculated with a single point analysis at the UB3LYP/6-311+G\*\* level. Simulations of the EPR spectra were performed with Easy Spin software for Matlab.

**Synthesis of 6:** A solution of  $\text{H}_2\text{SO}_4$  (70  $\mu\text{L}$ , 1.299 mmol, 3 equiv.) in *t*BuOAc (4 mL) was added dropwise over 10 min to a pale yellow solution of **5** (400 mg, 0.433 mmol, 1 equiv.) in *t*BuOAc (30 mL) at 0 °C. A white precipitate formed during the addition of the sulfuric acid. The heterogeneous solution was stirred at 0 °C for 10 min, and then for 1 h at room temp. The reaction was quenched with  $\text{NaHCO}_3$  (saturated aq.), and the mixture was vigorously stirred until the white-yellow solid had completely dissolved. EtOAc (15 mL) was added, and the layers were separated. The aqueous layer was extracted with EtOAc (3  $\times$  20 mL). The combined organic layers were dried with  $\text{MgSO}_4$ , and filtered, and the solvent was removed under reduced pressure. The residue was purified by flash chromatography on deactivated silica gel. Starting material and impurities were removed with  $\text{CH}_2\text{Cl}_2/\text{MeOH}$ , 9:1, then the product was eluted with  $\text{CH}_2\text{Cl}_2/\text{MeOH}/\text{Et}_3\text{N}$ , 89:10:1 to give **6** (169 mg, 47%) as a pale yellow oil.  $^1\text{H}$  NMR (500 MHz,  $\text{CDCl}_3$ ):  $\delta = 1.27$  (s, 9 H, 11-H), 1.90 (m, 2 H, 28-H), 2.19 (m, 2 H, 20-H), 2.69 (t,  $J = 6.3$  Hz, 2 H, 29-H), 2.74 (t,  $J = 7.5$  Hz, 2 H, 21-H), 2.80 (m, 2 H, 37-H), 2.92 (dd,  $J = 6.6$ , 14.0 Hz, 1 H, 7-H), 3.40 (m, 2 H, 27-H), 3.44 (t,  $J = 5.2$  Hz, 2 H, 36-H), 3.50–3.90 (m, 8 H, 32-H to 35-H), 4.00 (t,  $J = 6.4$  Hz, 2 H, 19-H), 4.09 (dd,  $J = 5.6$ , 6.4 Hz, 1 H, 8-H), 4.14 (br. s, 2 H, 31-H), 5.17 (br. s, 1 H, NH), 6.35 (d,  $J = 7.3$  Hz, 1 H, 23-H), 6.71 (d,  $J = 8.4$  Hz, 1 H, 3-H), 6.81 (dd,  $J = 2.1$ , 8.3 Hz, 1 H, 4-H), 7.06 (d,  $J = 7.2$  Hz, 1 H, 24-H), 7.54 (t,  $J = 7.8$  Hz, 1 H, 14-H), 7.72 (d,  $J = 7.7$  Hz, 1 H, 15-H), 7.94 (d,  $J = 7.9$  Hz, 1 H, 13-H), 8.02 (s, 1 H, 17-H), 8.10 (d,  $J = 2.0$  Hz, 1 H, 6-H), 9.00 (s, 1 H, NH) ppm.  $^{13}\text{C}$  NMR (125 MHz,  $\text{CDCl}_3$ ):  $\delta = 21.5$  (C-28), 26.5 (C-29), 27.8 (C-11), 29.2 (C-20), 33.8 (C-21), 38.8 (C-7), 41.7 (C-27, C-37), 57.5 (C-8), 68.0 (C-19), 70.3–71.3 (C-31 to C-35), 73.3 (C-36), 82.9 (C-10), 111.1 (C-3), 111.4 (C-23), 113.9 (C-25), 121.1 (C-6), 123.4 (q,  $J = 272.9$  Hz, C-18), 124.2 (q,  $J = 3.9$  Hz, C-17), 125.3 (C-4), 127.0 (C-1), 127.9 (C-5), 129.0 (q,  $J = 3.4$  Hz, C-15), 129.7 (C-14), 130.6 (C-13), 131.4 (q,  $J = 33.4$  Hz, C-16), 136.9 (C-24), 141.9 (C-12), 147.0 (C-2), 156.0 (C-26), 156.6 (C-22), 167.8 (C-30), 170.0 (C-9) ppm.  $^{19}\text{F}$  NMR (282 MHz,  $\text{CDCl}_3$ ):  $\delta = -63.30$  (s, 3 F, 18-F) ppm. HRMS (TOF ES<sup>+</sup>): calcd. for  $\text{C}_{39}\text{H}_{53}\text{F}_3\text{N}_5\text{O}_9\text{S}$  824.3516; found 824.3500.

**Synthesis of 8 and 9:** LiOH (10.6 mg, 0.444 mmol, 1 equiv.) in water (5 mL) was added to a stirred solution of **7** (490 mg, 0.444 mmol, 1 equiv.) in dioxane (15 mL). The mixture was heated at reflux for 20 h. The solvent was removed under reduced pressure, and EtOAc (20 mL) and  $\text{H}_2\text{SO}_4$  (1 M; 5 mL) were added. The layers were sepa-

rated, and the aqueous layer extracted with EtOAc (3 × 10 mL). The combined organic layers were dried with MgSO<sub>4</sub>. The solvent was removed under reduced pressure, and the residue was purified by column chromatography on silica gel (CH<sub>2</sub>Cl<sub>2</sub> to CH<sub>2</sub>Cl<sub>2</sub>/MeOH, 7:3) to give recovered starting material (196 mg, 40%), and desired compound **8** (147 mg, 30%) as an orange solid. *R*<sub>f</sub>: 0.5 (CH<sub>2</sub>Cl<sub>2</sub>/MeOH, 9:1). <sup>1</sup>H NMR (500 MHz, CDCl<sub>3</sub>): δ = 1.45 (t, *J* = 7.10 Hz, 6 H, 10-H), 1.65–1.77 (several singlets, 36 H, 7-H), 4.44 (m, 4 H, 9-H), 6.79 (s, 1 H, OH) ppm. <sup>13</sup>C NMR (125 MHz, CDCl<sub>3</sub>): δ = 14.4 (C-10), 28.4 (C-7), 28.8 (C-7), 28.9 (C-7), 29.1 (C-7), 29.1 (C-7), 29.8 (C-7), 31.4 (C-7), 32.2 (C-7), 32.3 (C-7), 33.6 (C-7), 34.0 (C-7), 34.3 (C-7), 60.9 (C-6), 60.9 (C-6), 61.0 (C-6), 61.0 (C-6), 61.0 (C-6), 61.4 (C-6), 62.5 (C-9), 62.5 (C-9), 84.4 (C-1), 121.4 (3 C, C-Ar), 133.8 (C-Ar), 134.1 (C-Ar), 134.7 (C-Ar), 138.9 (C-Ar), 139.5 (C-Ar), 139.6 (C-Ar), 140.3 (C-Ar), 140.4 (C-Ar), 140.6 (C-Ar), 141.6 (C-Ar), 141.7 (C-Ar), 141.9 (C-Ar), 142.0 (C-Ar), 142.4 (C-Ar), 143.0 (C-Ar), 166.3 (C-8), 171.2 (C-11) ppm. HRMS (TOF ES<sup>+</sup>): calcd. for C<sub>44</sub>H<sub>47</sub>O<sub>7</sub>S<sub>12</sub> 1070.9970; found 1070.9915.

And finally dihydrolysed compound **9** (46 mg, 10%) as an orange solid. *R*<sub>f</sub>: 0.3 (CH<sub>2</sub>Cl<sub>2</sub>/MeOH, 7:3). <sup>1</sup>H NMR (500 MHz, [D<sub>6</sub>]DMSO): δ = 1.34 (t, *J* = 7.08 Hz, 3 H, 10-H), 1.54 (s, 3 H, 7-H), 1.54 (s, 3 H, 7-H), 1.57 (s, 3 H, 7-H), 1.58 (s, 6 H, 7-H), 1.62 (s, 3 H, 7-H), 1.63 (s, 3 H, 7-H), 1.64 (s, 9 H, 7-H), 1.69 (s, 3 H, 7-H), 1.70 (s, 3 H, 7-H), 4.33 (m, 2 H, 9-H), 6.76 (s, 1 H, OH) ppm. <sup>13</sup>C NMR (125 MHz, [D<sub>6</sub>]DMSO): δ = 14.0 (C-10), 27.4 (C-7), 27.5 (C-7), 27.9 (C-7), 28.0 (C-7), 28.7 (C-7), 29.7 (C-7), 30.5 (C-7), 31.8 (C-7), 32.1 (C-7), 34.2 (C-7), 34.2 (C-7), 24.4 (C-7), 59.2 (C-6), 59.5 (C-6), 59.7 (C-6), 59.9 (C-6), 60.4 (C-6), 60.7 (C-6), 62.1 (C-9), 83.5 (C-1), 120.6 (3 C, C-Ar), 130.0–145.0 (15 C, C-Ar), 165.3 (C-8), 169.6 (C-11) ppm. HRMS (TOF ES<sup>+</sup>): calcd. for C<sub>42</sub>H<sub>43</sub>O<sub>7</sub>S<sub>12</sub> 1042.9657; found 1042.9702.

**Synthesis of 11:** DIEA (23 μL, 0.137 mmol, 1 equiv.) was added to a stirred solution of **8** (147 mg, 0.137 mmol, 1 equiv.) in CH<sub>2</sub>Cl<sub>2</sub> (10 mL). The solution was cooled to –78 °C, and oxalyl chloride (59 μL, 0.685 mmol, 5 equiv.) was added. The red solution was stirred at –78 °C for 15 min, and then overnight at room temp. The solvent was removed under reduced pressure, and the residue was purified by elution through a short (5 cm) pad of silica gel (CH<sub>2</sub>Cl<sub>2</sub>) to give **11** (143 mg, 96%) as a red solid. <sup>1</sup>H NMR (500 MHz, CDCl<sub>3</sub>): δ = 1.47 (t, *J* = 8.10 Hz, 3 H, 10-H), 1.47 (t, *J* = 8.10 Hz, 3 H, 10-H), 1.66 (s, 3 H, 7-H), 1.67 (s, 6 H, 7-H), 1.68 (s, 3 H, 7-H), 1.70 (s, 3 H, 7-H), 1.72 (s, 3 H, 7-H), 1.75 (s, 3 H, 7-H), 1.77 (s, 9 H, 7-H), 1.79 (s, 3 H, 7-H), 1.80 (s, 3 H, 7-H), 1.80 (s, 3 H, 7-H), 4.44 (m, 4 H, 9-H), 6.78 (s, 1 H, OH) ppm. <sup>13</sup>C NMR (125 MHz, CDCl<sub>3</sub>): δ = 14.4 (C-10), 28.2 (C-7), 28.3 (C-7), 28.5 (C-7), 29.1 (C-7), 29.6 (C-7), 30.5 (C-7), 30.8 (C-7), 32.3 (C-7), 32.8 (C-7), 33.3 (C-7), 34.0 (C-7), 34.3 (C-7), 61.0 (C-6), 61.1 (C-6), 61.2 (C-6), 61.8 (C-6), 62.6 (C-9), 63.3 (C-6), 63.6 (C-6), 84.3 (C-1), 121.5 (3 C, C-Ar), 128.0 (C-Ar), 133.7 (C-Ar), 134.1 (C-Ar), 137.5 (C-Ar), 138.4 (C-Ar), 138.5 (C-Ar), 139.5 (C-Ar), 140.2 (C-Ar), 140.4 (C-Ar), 141.1 (C-Ar), 141.4 (C-Ar), 141.8 (C-Ar), 142.0 (C-Ar), 142.3 (C-Ar), 166.3 (C-8), 167.5 (C-11) ppm.

**Synthesis of 12:** Compound **6** (170 mg, 0.206 mmol, 1.6 equiv.) was dissolved in CH<sub>2</sub>Cl<sub>2</sub> (6 mL), and pyridine (16 μL, 0.206 mmol, 1.6 equiv.) and **11** (140 mg, 0.125 mmol, 1 equiv.) in CH<sub>2</sub>Cl<sub>2</sub> (1 mL) were added. The solution was stirred at room temp. for 24 h, then NH<sub>4</sub>Cl (saturated aq.; 3 mL) was added, and the layers were separated. NaHCO<sub>3</sub> (saturated aq.; 3 mL) was added to the organic phase, and the layers were separated. The aqueous phase was extracted with EtOAc (2 × 5 mL). The combined organic layers were dried with MgSO<sub>4</sub>, and the solvent was removed under reduced

pressure. The residue was purified by column chromatography on silica gel (acetone/EtOAc, 1:4 to 1:1) to give **12** (139 mg, 57%) as an orange solid. *R*<sub>f</sub>: 0.25 (EtOAc/acetone, 5:1). <sup>1</sup>H NMR (500 MHz, CDCl<sub>3</sub>): δ = 1.24 (s, 9 H, 30-H), 1.44 (t, *J* = 7.0 Hz, 6 H, 10-H), 1.61–1.76 (several singlets, 36 H, 7-H), 1.87 (m, 2 H, 46-H), 2.17 (m, 2 H, 39-H), 2.66 (t, *J* = 6.1 Hz, 2 H, 45-H), 2.73 (t, *J* = 7.3 Hz, 2 H, 40-H), 2.86 (dd, *J* = 7.0, 13.9 Hz, 1 H, 27-H), 2.98 (dd, *J* = 5.2, 13.9 Hz, 1 H, 27-H), 3.37 (m, 2 H, 47-H), 3.54–3.77 (m, 12 H, 17-H to 12-H), 3.98 (t, *J* = 6.1 Hz, 2 H, 38-H), 4.05 (m, 1 H, 27-H), 4.11 (s, 2 H, 18-H), 4.42 (m, 4 H, 9-H), 5.44 (s, 1 H, NH), 6.31 (d, *J* = 7.2 Hz, 1 H, 42-H), 6.68 (d, *J* = 8.3 Hz, 1 H, 24-H), 6.73 (s, 1 H, OH), 6.8 (dd, *J* = 1.7, 8.3 Hz, 1 H, 23-H), 7.05 (d, *J* = 7.2 Hz, 1 H, 43-H), 7.53 (t, *J* = 7.9 Hz, 1 H, 33-H), 7.71 (d, *J* = 7.7 Hz, 1 H, 34-H), 7.91 (d, *J* = 8.0 Hz, 32-H), 7.99 (s, 1 H, 36-H), 8.12 (s, 1 H, 21-H), 8.94 (s, 1 H, NH) ppm. <sup>13</sup>C NMR (125 MHz, CDCl<sub>3</sub>): δ = 14.4 (C-10), 21.0 (C-46), 26.3 (C-45), 27.7 (C-7), 27.8 (C-30), 29.3 (C-7), 29.4 (C-7), 29.7 (C-7), 30.5 (C-7), 31.8 (C-7), 32.7 (C-7), 32.7 (C-40), 33.0 (C-7), 33.8 (C-7), 34.4 (C-7), 34.9 (C-7), 38.9 (C-26), 39.8 (C-12), 41.5 (C-47), 57.3 (C-27), 60.9 (C-6), 61.1 (C-6), 61.3 (C-6), 61.9 (C-6), 62.0 (C-6), 62.6 (C-9), 67.6 (C-38), 69.5–71.5 (6 peaks, C18 to C13), 83.1 (C-29), 84.3 (C-1), 111.1 (C-24), 111.1 (C-42), 120.8 (C-21), 121.4 (3 C-Ar), 123.3 (q, *J* = 273.1 Hz, C-37), 124.3 (q, *J* = 3.2 Hz, C-36), 125.3 (C-23), 127.0 (C-20), 127.7 (C-22), 129.2 (q, *J* = 2.8 Hz, C-34), 129.8 (C-33), 130.7 (C-32), 131.5 (q, *J* = 33.6 Hz, C-35), 131.8 (C-Ar), 134.5 (C-Ar), 136.7 (C-Ar), 137.2 (C-Ar), 137.8 (C-43), 138.1 (C-Ar), 139.3 (C-Ar), 140.4–142.2 (9 peaks, 8 C-Ar, C-31), 146.7 (C-44), 155.1 (C-41, C-48), 166.3 (C-8), 166.3 (C-8), 167.1 (C-11), 167.6 (C-19), 169.9 (C-28) ppm. HRMS (TOF ES<sup>+</sup>): calcd. for C<sub>83</sub>H<sub>99</sub>N<sub>5</sub>O<sub>15</sub>F<sub>3</sub>S<sub>13</sub> 1878.3459; found 1878.3258.

**Synthesis of 13:** Compound **12** (70 mg, 0.037 mmol) was dissolved in TFA (10 mL). The solution was stirred for 2 h at room temp., and then the TFA was removed under reduced pressure. The crude product was purified by semi-preparative HPLC to give pure **13** (27 mg, 40%). The conditions of purification were as follows: Column XBridge 10 × 100 mm 5 μm, equipped with a guard column 10 × 20 mm 5 μm. UV detection at 485 nm. Flow rate 5 mL/min. Isocratic elution with MeCN/H<sub>2</sub>O/H<sub>2</sub>O containing TFA (1%), 70:20:10. The fraction corresponding to the peak maximum was collected. HRMS (TOF ES<sup>+</sup>): calcd. for C<sub>79</sub>H<sub>90</sub>N<sub>5</sub>O<sub>14</sub>F<sub>3</sub>S<sub>13</sub> 1805.28001; found 1805.27957.

**Synthesis of 14:** **13** (15 mg, 0.038 mmol) was dissolved in dioxane (2 mL). LiOH (1 M aq.; 1 mL) was added, and the solution was stirred overnight. HCl (1 M aq.; 2 mL) and EtOAc (3 mL) were added, and the layers were separated. The aqueous layer was extracted with EtOAc (3 × 6 mL). The combined organic layers were dried with MgSO<sub>4</sub>, and filtered, and the solvent was removed under reduced pressure. The crude product was purified by semi-preparative HPLC to give **14** (9.3 mg, 29%). The conditions of purification were as follows: Column XBridge 10 × 100 mm 5 μm, equipped with a guard column 10 × 20 mm 5 μm. UV detection at 486 nm. Gradient elution: see Table 2. The fraction corresponding to the

Table 2. Gradient elution.

Time [min]	Flow [mL/min]	MeOH [%]	H <sub>2</sub> O [%]	H <sub>2</sub> O (1% TFA) [%]
0	5	68	22	10
10	5	68	22	10
11	5	90	0	10
14	5	90	0	10
14.1	5	68	22	10

peak maximum was collected. HRMS (TOF ES<sup>+</sup>): calcd. for C<sub>75</sub>H<sub>82</sub>N<sub>5</sub>O<sub>14</sub>F<sub>3</sub>S<sub>13</sub> 1749.21741; found 1749.21683.

**Supporting Information** (see footnote on the first page of this article): Synthetic procedure for compound **7**; analytical HPLC data for radicals **13** and **14**; simulation parameters of calculated EPR spectra; and NMR spectra of nonparamagnetic compounds.

## Acknowledgments

This work was supported by the Université catholique de Louvain (UCL) and the Fond de la Recherche Scientifique (FRS-FNRS, Belgium). J. M.-B. is a senior research associate of the FRS-FNRS. The authors gratefully acknowledge Laurent Collard for his help with HPLC purifications, as well as Dr. Cecile Le Duff, Prof. Raphaël Robiette, and Martin Poncelet for helpful discussions. Sabrina Devouge is acknowledged for the preparation of the manuscript, and Keyton L. Clayson for proof reading. Computational resources were provided by the supercomputing facilities of the Université catholique de Louvain (CISM/UCL) and the Consortium des Équipements de Calcul Intensif en Fédération Wallonie Bruxelles (CÉCI), funded by the Fond de la Recherche Scientifique (FRS-FNRS, Belgium) under convention 2.5020.11.

- [1] M. C. Krishna, N. Devasahayam, J. A. Cook, S. Subramanian, P. Kuppusamy, J. B. Mitchell, *ILAR J.* **2001**, *42*, 209–218.
- [2] E. Vanea, N. Charlier, J. DeWever, M. Dinguzli, O. Feron, J.-F. Baurain, B. Gallez, *NMR Biomed.* **2008**, *21*, 296–300.
- [3] B. Gallez, C. Baudelet, B. F. Jordan, *NMR Biomed.* **2004**, *17*, 240–262.
- [4] J. H. Ardenkjær-Larsen, I. Laursen, I. Leunbach, G. Ehnholm, L. G. Wistrand, J. S. Petersson, K. Golman, *J. Magn. Reson.* **1998**, *133*, 1–12.
- [5] B. Driesschaert, P. Levêque, B. Gallez, J. Marchand-Brynaert, *Tetrahedron Lett.* **2013**, *54*, 5924–5926.
- [6] a) B. Gallez, V. Lacour, R. Demeure, R. Debuyst, F. Dejehet, J. L. De Keyser, P. Dumont, *Magn. Reson. Imaging* **1994**, *12*, 61–69; b) B. Gallez, R. Debuyst, R. Demeure, F. Dejehet, C. Grandin, B. Van Beers, H. Taper, J. Pringot, P. Dumont, *Magn. Reson. Med.* **1993**, *30*, 592–599.
- [7] a) J. Liu, M. Zhao, C. Wang, S. Peng, *Bioorg. Med. Chem. Lett.* **2003**, *13*, 4065–4069; b) J. Liu, M. Zhao, C. Wang, S. Peng, *Bioorg. Med. Chem.* **2008**, *16*, 4019–4028.
- [8] a) A. A. Bobko, I. Dhimitruka, J. L. Zweier, V. V. Khramtsov, *J. Am. Chem. Soc.* **2007**, *129*, 72440–72441; b) I. Dhimitruka, A. A. Bobko, C. M. Hadad, J. L. Zweier, V. V. Khramtsov, *J. Am. Chem. Soc.* **2008**, *130*, 10780–10787; c) O. Y. Rogozhnikova, V. G. Vasiliev, T. I. Troitskaya, D. V. Trukhin, T. V. Mikhailina, H. J. Halpern, V. M. Tormyshev, *Eur. J. Org. Chem.* **2013**, 3347–3355.
- [9] J. S. Desgrosellier, D. A. Cheresch, *Nat. Rev. Cancer* **2010**, *10*, 9–22.
- [10] S. D. Robinson, K. M. Hodivala-Dilke, *Curr. Opin. Cell Biol.* **2011**, *23*, 630–637.
- [11] J. F. Marshall, S. A. Nesbitt, M. H. Helfrich, M. A. Horton, K. Polakova, I. R. Hart, *Int. J. Cancer* **1991**, *49*, 924–931.
- [12] a) D. Cox, M. Brennan, N. Moran, *Nat. Rev. Drug Discovery* **2010**, *9*, 804–820; b) A. Perdih, M. Sollner Dolenc, *Curr. Med. Chem.* **2010**, *17*, 2371–2392.
- [13] M. Barczyk, S. Carracedo, D. Gullberg, *Cell Tissue Res.* **2010**, *339*, 269–280.
- [14] M. A. Dechantsreiter, E. Planker, B. Mathä, E. Lohof, G. Hölzemann, A. Jonczyk, S. L. Goodman, H. Kessler, *J. Med. Chem.* **1999**, *42*, 3033–3040.
- [15] K.-E. Gottschalk, H. Kessler, *Angew. Chem. Int. Ed.* **2002**, *41*, 3767–3774; *Angew. Chem.* **2002**, *114*, 3919–3927.
- [16] K. Chen, X. Chen, *Theranostics* **2011**, *1*, 189–200.
- [17] J.-P. Xiong, T. Stehle, R. Zhang, A. Joachimiak, M. Frech, S. L. Goodman, M. A. Arnaout, *Science* **2002**, *296*, 151–155.
- [18] V. Rerat, G. Dive, A. A. Cordi, G. C. Tucker, R. Bareille, J. I. Amédée, L. Bordenave, J. Marchand-Brynaert, *J. Med. Chem.* **2009**, *52*, 7029–7043.
- [19] M. Remy, R. Bareille, V. Rerat, C. Bourget, J. Marchand-Brynaert, L. Bordenave, *J. Biomater. Sci. Polym. Ed.* **2013**, *24*, 269–286.
- [20] V. Rerat, S. Laurent, C. Burtea, B. Driesschaert, V. Pourcelle, L. Vander Elst, R. N. Muller, J. Marchand-Brynaert, *Bioorg. Med. Chem. Lett.* **2010**, *20*, 1861–1865.
- [21] L. S. Lin, T. Lanza Jr., S. E. de Laszlo, Q. Truong, T. Kamenecka, W. K. Hagmann, *Tetrahedron Lett.* **2000**, *41*, 7013–7016.
- [22] T. J. Reddy, T. Iwama, H. J. Halpern, V. H. Rawal, *J. Org. Chem.* **2002**, *67*, 4635–4639.
- [23] a) I. Dhimitruka, M. Velayutham, A. A. Bobko, V. V. Khramtsov, F. A. Villamena, C. M. Hadad, J. L. Zweier, *Bioorg. Med. Chem. Lett.* **2007**, *17*, 6801–6805; b) B. Driesschaert, R. Robiette, C. S. Le Duff, L. Collard, K. Robeyns, B. Gallez, J. Marchand-Brynaert, *J. Org. Chem.* **2012**, *77*, 6517–6525.
- [24] S. Stoll, A. Schweiger, *J. Magn. Reson.* **2006**, *178*, 42–55.
- [25] M. K. Bowman, C. Mailer, H. J. Halpern, *J. Magn. Reson.* **2005**, *172*, 254–267.
- [26] A. K. Hui, B. H. Armstrong, A. A. Wray, *J. Quant. Spectrosc. Radiat. Transfer* **1978**, *19*, 509–516.
- [27] M. Schottelius, B. Laufer, H. Kessler, H.-J. Wester, *Acc. Chem. Res.* **2009**, *42*, 969–980.
- [28] Z. Yang, Y. Liu, P. Borbat, J. L. Zweier, J. H. Freed, W. L. Hubbell, *J. Am. Chem. Soc.* **2012**, *134*, 9950–9952.
- [29] M. J. Frisch, G. W. Trucks, H. B. Schlegel, G. E. Scuseria, M. A. Robb, J. R. Cheeseman, G. Scalmani, V. Barone, B. Mennucci, G. A. Petersson, H. Nakatsuji, M. Caricato, X. Li, H. P. Hratchian, A. F. Izmaylov, J. Bloino, G. Zheng, J. L. Sonnenberg, M. Hada, M. Ehara, K. Toyota, R. Fukuda, J. Hasegawa, M. Ishida, T. Nakajima, Y. Honda, O. Kitao, H. Nakai, T. Vreven, J. A. Montgomery Jr., J. E. Peralta, F. Ogliaro, M. Bearpark, J. J. Heyd, E. Brothers, K. N. Kudin, V. N. Staroverov, R. Kobayashi, J. Normand, K. Raghavachari, A. Rendell, J. C. Burant, S. S. Iyengar, J. Tomasi, M. Cossi, N. Rega, J. M. Millam, M. Klene, J. E. Knox, J. B. Cross, V. Bakken, C. Adamo, J. Jaramillo, R. Gomperts, R. E. Stratmann, O. Yazyev, A. J. Austin, R. Cammi, C. Pomelli, J. W. Ochterski, R. L. Martin, K. Morokuma, V. G. Zakrzewski, G. A. Voth, P. Salvador, J. J. Dannenberg, S. Dapprich, A. D. Daniels, O. Farkas, J. B. Foresman, J. V. Ortiz, J. Cioslowski, D. J. Fox, *Gaussian 09, Revision B.01*, Gaussian, Inc., Wallingford CT, **2009**.

Received: August 7, 2014

Published Online: November 14, 2014